

Influence of hydrogen passivation on majority and minority charge carrier mobilities in ribbon silicon

Giso Hahn*, Patric Geiger, Detlef Sontag, Peter Fath, Ernst Bucher

Department of Physics, University of Konstanz, P.O. Box X916, 78457 Konstanz, Germany

Abstract

Multicrystalline silicon materials and ribbons in particular contain a higher amount of defects as compared to monocrystalline silicon, which have to be passivated during solar cell processing in order to reach satisfactory cell efficiencies. Within the solar cell process, this is usually carried out via the deposition of a hydrogen-rich SiN_x layer and a following firing step. During passivation, the electronic properties of the materials (conductivity, mobility) can change which might have an influence on the optimised parameters like emitter sheet resistance and grid geometry. This paper deals with the impact of hydrogen passivation on the electronic properties of majority and minority charge carriers in ribbon silicon materials. Majority charge carrier mobilities resulting from Hall measurements are strongly increasing after hydrogenation especially at temperatures below 300 K. Even at room temperature, changes in mobility up to a factor of 2 have been observed. For the determination of minority charge carrier mobilities in processed solar cells, a new method is presented based on spatially resolved internal quantum efficiency and lifetime measurements. It allows the calculation of mapped mobilities especially in materials showing small diffusion lengths. The same reductions in mobility of a factor 2–3 as compared to monocrystalline silicon for both majority and minority charge carriers could be detected in RGS silicon. © 2002 Elsevier Science B.V. All rights reserved.

Keywords: Ribbon; Multicrystalline; Silicon; RGS; EFG; String ribbon; Mobility; Majority carrier; Minority carrier; Hydrogen; Lifetime; Diffusion length

*Corresponding author. Fax: 49-7531-88-3895.
E-mail address: giso.hahn@uni-konstanz.de (G. Hahn).

1. Silicon Ribbons

For this study, we have chosen three p-type ribbon silicon materials which are found in different stages of development. Edge-defined film-fed growth (EFG) [1] from ASE has already been produced commercially for a longer time, string ribbon [2] by Evergreen Solar just made the step from pilot to mass production, ribbon growth on substrate (RGS) [3] by Bayer AG is still in the phase of development with a large-scale production machine under construction at the moment. For all materials wafering costs are minimised by avoiding ingot casting and sawing losses during subsequent wafering of the ingot. For RGS the very fast production rate (one wafer per second) can lead to even higher reductions in wafering costs. The method chosen for passivation in this study is the microwave-induced remote hydrogen plasma (MIRHP) passivation technique, which turned out to be very effective in former studies for multicrystalline as well as ribbon silicon materials in particular [4,5].

2. Majority charge carrier mobilities

Electronic properties of majority charge carriers (mobility and concentration) have been investigated by temperature-dependent Hall measurements in van der Pauw geometry [6] between 50 and 400 K before and after H-passivation (Fig. 1). For this investigation, we used two neighbouring 1 cm^2 samples originating from the same wafer. One was measured in the as-grown state, the other after a MIRHP passivation step. For all as-grown materials under investigation, a drop in Hall mobility $\mu_{H,p}$ in the low-temperature range (100–200 K) can be observed, leading to a minimum which is not observed in monocrystalline FZ silicon chosen as a reference material. This might be caused by acceptor-like traps at extended defects [7].

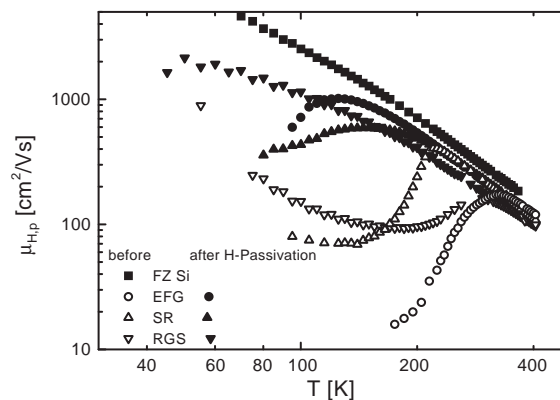


Fig. 1. Majority charge carrier Hall mobilities of p-type ribbon silicon wafers. The observed minimum between 100 and 200 K disappears after H-passivation.

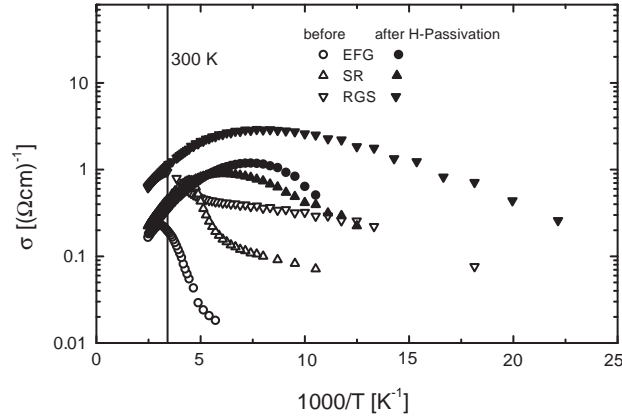


Fig. 2. Conductivity σ of hydrogenated and unhydrogenated silicon ribbons. The higher mobility after H-passivation leads to an increased conductivity.

Additionally, mobilities at room temperature are significantly lower than in the reference. For RGS this can be up to a factor of 3 ($150 \text{ cm}^2/\text{V s}$ as compared to $400 \text{ cm}^2/\text{V s}$ for mono-Si of the same resistivity [8]).

It could be shown that hole mobilities strongly increase between 100 and 200 K after H-passivation in all ribbon materials, causing the minimum to disappear. This leads to an increase in conductivity σ

$$\sigma \approx ep\mu_{H,p} \quad (1)$$

even at room temperature while carrier concentration p remains constant (Fig. 2). Up to two times higher σ values could be detected in hydrogenated EFG wafers at 300 K as compared to the as-grown wafer [9]. However, mobilities at room temperature are still lower than in the reference caused by a higher concentration of uncharged defects (e.g. dislocations).

3. Mapped minority charge carrier mobilities

3.1. Experimental approach

Minority charge carrier properties have been investigated on finished solar cell structures. Effective values of the diffusion length (L_{eff}) could be determined by a spectrally resolved internal quantum efficiency (IQE) mapping of the cell and fits on the obtained data using the method proposed by Basore [10]. Later the metal grid as well as the emitter was removed and the surfaces have been passivated. The bulk lifetime (τ_b) was mapped using photoconductivity decay detected by microwave reflection (μ -PCD, low injection). Assuming that L_{eff} equals the bulk diffusion length L_{diff} , which holds true especially for materials with diffusion lengths being small in

comparison to the cell thickness ($\sim 300 \mu\text{m}$), the minority charge carrier diffusion constant D_n can be calculated from

$$L_{\text{diff}} = \sqrt{D_n \tau_b}. \quad (2)$$

As D_n is proportional to the drift mobility μ_n of the electrons (minorities in p-type material) via

$$\mu_n = \frac{k_B T}{q} D_n, \quad (3)$$

we end up with a drift mobility mapping of the minority charge carriers.

3.2. Results

The results of this procedure for an H-passivated RGS solar cell can be seen in Fig. 3. On top, the L_{eff} map of the solar cell is shown. Note the grid fingers and the white spots with apparently high L_{eff} . The spatially resolved recombination inside the wafer is given by the τ_b map (middle). Combining the two maps according to Eqs. (2) and (3) results in a map of D_n or μ_n (bottom).

The mean value for μ_n of $450 \text{ cm}^2/\text{V s}$ (or $12 \text{ cm}^2/\text{s}$ for D_n) is a factor 2–3 lower than the values for mono-Si of the same resistivity at room temperature ($1040 \text{ cm}^2/\text{V s}$ or $27 \text{ cm}^2/\text{s}$ [8]). This is the same reduction as detected for majority carriers. Therefore at 300 K, we conclude that majority and minority charge carriers in RGS are dominated by the same scattering mechanisms.

In most areas a high/low value for L_{eff} is coupled with a high/low τ_b (e.g. upper circle). This leads to a distribution of μ_n , which seems not to be linked directly to the recombination strength. Or in other words, areas showing increased recombination do not necessarily result in increased scattering.

However, some areas of high L_{eff} but average τ_b show μ_n values far above $1040 \text{ cm}^2/\text{V s}$ (e.g. lower circle). In these small well-defined areas the fit to obtain L_{eff} led to wrong results caused by a 3-d emitter structure. The fit algorithm proposed in Ref. [10] can only be applied for a planar emitter structure. This is another hint for the existence of current collecting channels in RGS material [11].

3.3. Discussion

The results shown for RGS silicon reveal the facilities possible with this new technique. Due to the mapping character inhomogeneities within the sample can be detected, which is important for ribbon silicon materials in particular. Areas with a non-planar emitter structure can be detected as well. The maximum resolution is $100 \mu\text{m}$ (step size for $\mu\text{-PCD}$ measurement) with a diameter of the $\mu\text{-PCD}$ laser beam spot of $\sim 0.8 \text{ mm}$.

At the moment the application of this technique is restricted to areas of quite small L_{diff} . Therefore, it was not possible to map the whole cell area without getting a significant error in the determination of L_{diff} for other materials apart from RGS. But areas with small L_{diff} could be measured correctly.

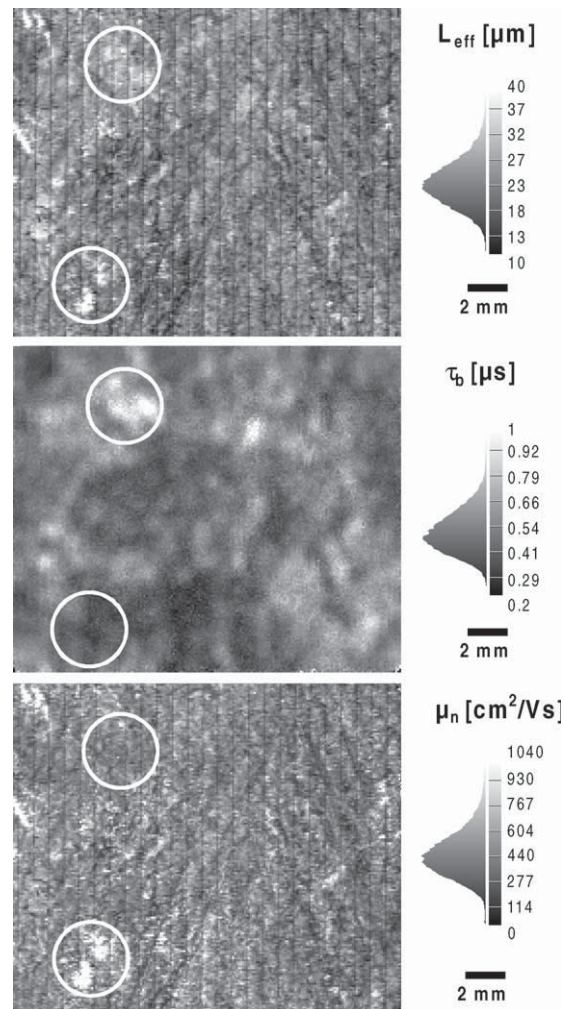


Fig. 3. Diffusion lengths of an RGS solar cell from IQE mapping (top), bulk lifetimes from μ -PCD (middle) and the resulting map for minority charge carrier mobility (bottom).

First comparative measurements have been carried out on EFG material with and without H-passivation in areas of small L_{diff} (same cell before and after passivation). In these first tests no significant change in mobility caused by hydrogenation could be observed, but this might be due to the limited number of suited measurement points mainly around grain boundaries causing a poor statistic. The method is described in more detail in Ref. [12].

Another interesting option for future investigations would be the temperature-dependant determination of minority carrier mobilities. For this purpose, a temperature control has to be developed for mapped lifetime (τ_b) as well as IQE

(L_{diff}) measurements. Using this additional information a more detailed comparison with the temperature-dependant majority Hall mobilities could be obtained.

4. Summary

The influence of hydrogenation on majority charge carrier mobilities has been investigated for three ribbon silicon materials. A significant drop in mobility in the temperature range of 100–200 K for all as-grown ribbons disappears in hydrogenated samples originating from the same wafer. For EFG the hydrogenated sample showed a significantly higher conductivity at 300 K (factor of 2). Nevertheless, mobilities at room temperature after hydrogenation are still lower than in monocrystalline silicon.

Mapped minority charge carrier mobilities have been determined using a new technique based on IQE and lifetime measurements. The application of this technique is restricted to materials/areas of L_{diff} being small as compared to the cell thickness at the moment, but works well in the case of RGS. Mean values for minority charge carriers demonstrate the same reduction in mobility as detected for majority carriers. Additionally, well-defined areas of a non-planar emitter structure could be detected in RGS with this technique. As a first result, no change in mobility after hydrogenation was observed for EFG, but this might be caused by the poor statistic, because only areas with small L_{diff} around grain boundaries could be evaluated yet.

Acknowledgements

We would like to thank T. Pernau for software support. Part of this work was financed by the German BMWi under contract number 0329858J.

References

- [1] F.V. Wald, in: H.C. Freyhardt (Ed.), *Crystals: Growth, Properties and Applications*, Vol. 5, Springer, Berlin, Germany, 1981.
- [2] W.M. Sachs, D. Ely, J. Serdy, Edge stabilized ribbon (ESR) growth of silicon for low cost photovoltaics, *J. Crystal Growth* 82 (1987) 117–121.
- [3] H. Lange, I.A. Schwirtlich, Ribbon growth on substrate (RGS)—a new approach to high speed growth of silicon ribbons for photovoltaics, *J. Crystal Growth* 104 (1990) 108–112.
- [4] M. Spiegel, P. Fath, K. Peter, B. Buck, G. Willeke, E. Bucher, Detailed study on microwave induced remote hydrogen plasma passivation of multicrystalline silicon, *Proceedings of the 13th EC PVSEC*, Nizza, 1995, pp. 421–424.
- [5] G. Hahn, W. Jooss, M. Spiegel, P. Fath, G. Willeke, E. Bucher, Improvement of mc Si solar cells by Al-gettering and hydrogen passivation, *Proceedings of the 26th IEEE PVSC*, Anaheim, 1997, pp. 75–78.
- [6] L.J. van der Pauw, A method of measuring specific resistivity and Hall effect of discs of arbitrary shape, *Philips Res. Rep.* 13 (1) (1958) 1–9.

- [7] H. Nussbaumer, F.P. Baumgartner, G. Willeke, E. Bucher, Hall mobility minimum of temperature dependence in polycrystalline silicon, *J. Appl. Phys.* 83 (1) (1998) 292–296.
- [8] A.B. Sproul, M.A. Green, A.W. Stephens, Accurate determination of minority carrier- and lattice scattering-mobility in silicon from photoconductance decay, *J. Appl. Phys.* 72 (9) (1992) 4161–4171.
- [9] G. Hahn, P. Geiger, P. Fath, E. Bucher, Hydrogen passivation of ribbon silicon—electronic properties and solar cell results, *Proceedings of the 28th IEEE PVSC, Anchorage, 2000*, pp. 95–98.
- [10] P.A. Basore, Numerical modeling of textured silicon solar cells using PC1D, *IEEE Trans. Electron Dev.* ED-37 (1990) 337–343.
- [11] C. Haessler, H.-U. Hoefs, S. Thurm, O. Breitenstein, M. Langenkamp, Electronic activity of inversion channels: exceptionally high short circuit currents $> 30 \text{ mA/cm}^2$ on small grain ribbon growth on substrate (RGS) silicon, *Proceedings of the 16th EC PVSEC, Glasgow, 2000*, pp. 1352–1355.
- [12] D. Sontag, G. Hahn, P. Fath, E. Bucher, Two dimensional resolution of minority carrier diffusion constants in different silicon materials, *E-MRS 2001 Spring Meeting, Strasbourg, 2001, Solar Energy Mater. Solar Cells*, in press.